RADAR STATISTICAL RECONNAISSANCE OF THE 2016 INSIGHT LANDING SITES. C. Grima[1] and D. D. Blankenship[1], [1]University of Texas Institute for Geophysics, J.J. Pickle Research Campus, Bldg. 196, 10100 Burnet Rd. (R2200), Austin, TX 78758. cyril.grima@gmail.com

Introduction: The NASA's InSight (Interior Exploration using Seismic Investigations, Geodesy and Heat Transport) Lander is scheduled for launch and Mars landing in March and September 2016, respectively. From 16 landing sites defined in 2012, the selection has been narrowed to 4 potential ellipses based on engineering criteria [1]. The landing site selection process is achieved through a combination of various orbital remote-sensing technologies (e.g. laser altimetry, imagery, spectro-imagery, spectroscopy, thermal sensing) to assess the terrain relief, surface cohesiveness, rock height and rock abundance [2]. We will present and discuss the novel Radar Statistical Reconnaissance (RSR) technique applied to the active 20-MHz Shallow Radar (SHARAD) instrument [3] to support the InSight landing site selection.

Shallow Radar (SHARAD): SHARAD onboard the NASA's Mars Reconnaissance Orbiter (MRO) is an active nadir-looking instrument transmitting a 20-MHz central-frequency signal chirped over a 10-MHz bandwidth [3]. A fraction of the energy is partly scattered back and recorded at the antenna for each permittivity gradient (i.e. geologic discontinuities) along the propagation path until signal extinction, allowing for deep sounding down to ~1.5 km in clean water ice [4]. The atmosphere-surface echo is the first signal recorded by the antenna. Both the high dielectric contrast between these two media and the absence of volume scattering within the atmosphere, combine to give the echo a high signal-to-noise ratio. The radar surface return holds important information valuable for landing site selection since its amplitude depends on the surface composition, density and roughness.

Radar Statistical Reconnaissance (RSR): The RSR is a systematic method to extract and invert quantitative surface properties from the radar surface return. It has been recently demonstrated with the High Capability Radar Sounder (HiCARS, 60-MHz central frequency, 15-MHz bandwidth) airborne radar data in Antarctica [5, 6]. The RSR relies on a physical description of the surface echo assuming a stochastic behavior for the surface geometry. Analytically, the surface echo strength detected by the radar antenna is the summation of two fundamental components, the signal reflectance and scattering [e.g. 7]. The contribution of surface permittivity and deterministic structure (e.g. thin deposit or layering) is dominant in the reflectance, while scattering is mainly a function of the surface roughness and random internal geometries of the near-surface (e.g. a pile of blocks from a collapsed terrain).

Firstly, the RSR aims to extract the reflected and scattered components of the signal by best-fitting the histogram of ~ 1000 surface echo amplitudes with a theoretical stochastic model (homodyne K-statistics [8]). The correlation coefficient of this fit is a confidence factor to estimate the terrain compliance to the model assumptions. The scattering, reflectance and correlation coefficient give a first qualitative insight into the surface properties. Once deduced from the fit, they can be used in a backscattering model to produce a landing risk assessment indicator by considering the following surface criteria that affects the signal: Root mean square (RMS) heights, RMS slopes, correlation length, roughness homogeneity/stationarity over the landing ellipse, and soil porosity [5].

RSR application to SHARAD data: SHARAD observation tracks are North-South oriented and spaced from 1 to 100 km over the InSight landing region (Figure 1). The MRO ground speed combined with an effective pulse repetition frequency (PRF after onboard pulse pre-summing) of ~175 Hz provides surface sampling every ~ 20 m along-track. It follows that the typical sampled space over which the surface statistical properties can be retrieved (~1000 successive surface echoes) is ~20 km, resolving the length of the East-West oriented 139 km × 27 km ellipses considered for the 2016 InSight lander [9]. SHARAD can achieve ~ 50 dB of signal to noise ratio from a specular and conductive surface, promising a theoretical sensitivity to surface Root Mean Square (RMS) heights from 0.01 m to 3 m over a horizontal scale (baseline) ranging from one to few wavelengths (one SHARAD wavelength is 15 m) [5]. Conversely, the radar signal is expected be sensitive to the surface correlation length and RMS slope with baselines in the range of the pulse limited footprint (~ 5 km in diameter across-track) [10].

We will present the RSR application to the SHARAD data over the 16 preselected landing ellipses for the InSight lander. The results in terms of surface properties and landing risk assessment will be validated by comparison to other remote sensing data used for the 2012 landing site selection step [13]. A detailed landing risk assessment will be presented for the 4 landing ellipses still under consideration. The obtained results will also illustrate the RSR capabilities to support other future landed missions, especially the ESA's ExoMars 2018 and the NASA's Mars 2020 rover.

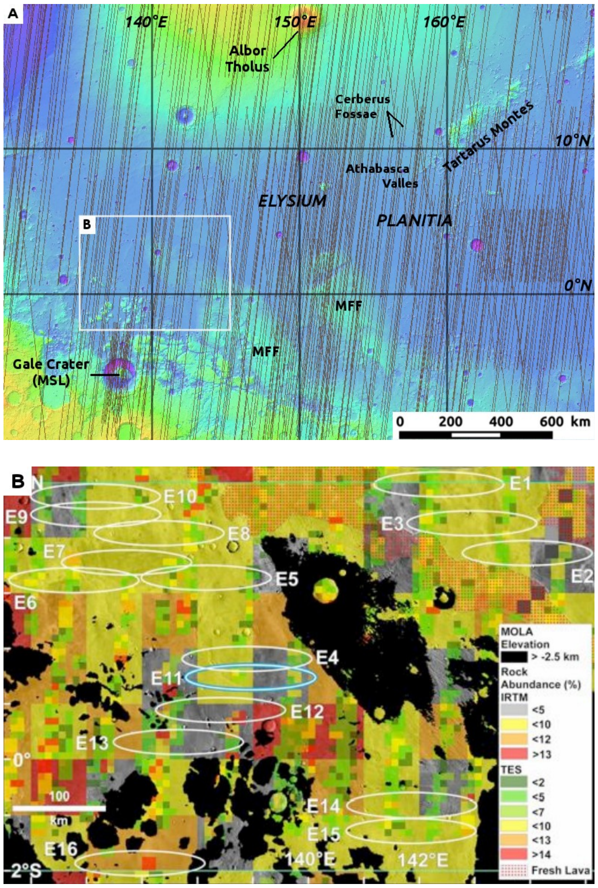

Fig 1. A. SHARAD orbit tracks over Elysium Planitia. The background is the Mars Orbiter Laser Altimeter (MOLA) shaded relief (red: high, blue: low). B. Initial 16 InSight landing site ellipses in Elysium Planitia with elevation limit (black), young lava from Athabasca Valles, and rock abundance determined by the InSight landing site working group. The last 4 ellipses considered for landing are E5, E8, E9, and E17 From [13].

References:

[1] Golombek M. et al., (2014) *LPSC XLV*, Abstract #1499. [2] Ball A. et al., (2007) *Cambridge University Press* [3] Seu et al. (2007) *JGR, 112*, E05S05. [4] Grima C. et al. (2009) *GRL, 36*, L03203. [5] Grima C. et al., (2014) *PSS, 103*, 191-204. [6] Grima C. et al. (2014) *GRL, 41(19)*, 6787-6794. [7] Ishimaru A. (1999) *Wiley-IEEE Pres*s. [8] Destrempes F. and Cloutier G., (2010) *Ultrasound Med Biol, 36(7)*, 1037-1051. [9] Golombek M. et al. (2013) *LPSC XVIV*, Abstract #1691. [10] Grima et al. (2012) *Icarus 220*, 84-99.